Heat transfer intensification of NEPCM-water suspension filled heat sink cavity with notches cooling tubes by applying the electric field

Mehdi Hashemi-Tilehnoee [1, *], Seyyed Masoud Seyyedi [2,3], Elena Palomo del Barrio [1,4], Mohsen Sharifpur [5,6,*]

[1] Centre for Cooperative Research on Alternative Energies (CIC energiGUNE), Basque Research and Technology Alliance (BRTA), Alava Technology Park, Albert Einstein 48, 01510 Vitoria-Gasteiz, Spain

[2] Department of Mechanical Engineering, Aliabad Katoul Branch, Islamic Azad University, Aliabad Katoul, Iran

[3] Energy Research Center, Aliabad Katoul Branch, Islamic Azad University, Aliabad Katoul, Iran

[4] IKERBASQUE Basque Foundation for Science, Plaza Euskadi 5, 48009 Bilbao, Spain

[5] Department of Mechanical and Aeronautical Engineering, University of Pretoria, Pretoria 0002, South Africa

[6] Department of Medical Research, China Medical University Hospital, China Medical University, Taichung, Taiwan

*Corresponding author:(M. Hashemi-Tilehnoee) mhashemi@cicenergigune.com

(M. Sharifpur) mohsen.sharifpur@up.ac.za

Highlights

- The NEPCM-filled complex cavity was numerically studied in the presence of an electric field.
- The electric field enhanced the heat transfer if applied in a valid setup.
- The Be_{ave} increases with the electric field and diminishes with the *Ra*.
- The ANSYS Fluent can solve complex problems in the presence of an electric field.

Abstract:

The effects of an electric field on heat transfer, free convection, and entropy generation of nano-encapsulated phase change material (NEPCM) dissolved in water in a complex inclined chamber are studied. The enclosure consists of a rectangular cavity heated from below and the remaining walls are considered adiabatic. The fluid is cooled by eight cooling tubes, each with four notches. The effects of the electric field, inclination angle ($\zeta = 45°$ and $\zeta = 90°$), and Rayleigh number (Ra=10^3, 10^4, and 10^5) in equal concentration of NEPCM (ϕ = 2%) are studied using ANSYS Fluent CFD code. The dimensionless form of fluid governing equations, electric potential equation, electric charge density equation, and entropy generation equation are used to set the primitive parameters. Grid verification and validation tests are performed to ensure the reliability of the solution. Calculations show that with increasing Ra, the average Nusselt number (Nu_{ave}) decreases from $\zeta = 45°$ to 90°, but when an electric field is applied, the results are reversed. As the Rayleigh number increases in conjunction with the electric field, the buoyancy effect becomes more pronounced. Furthermore, owing to its high heat transfer potential and lowest irreversibility, the straight cavity ($\zeta = 90°$) is desirable at Ra=10^5.

Keywords: Natural convection, NEPCM, Entropy generation, Electric field, Ansys Fluent.

1.Introduction

Thermal management of electronic devices is one of the requirements of the electronics industry, which has grown a lot in recent years. Due to increased performance and reduced size, the heat generated by new electronic equipment has increased dramatically. As a result, several studies have been conducted on micro heat sinks. They focused on the use of pin fins, their arrangement, and their cross-sectional shape. Apart from heat sinks, latent thermal energy storage has been proposed as a potential candidate because it stores energy in the form of latent heat. Materials used to store latent heat energy are known as phase change materials (PCM). The motivation for this study is to introduce NEPCM into the water to increase the heat storage capability. Then analyze free convection inside a closed heat exchanger acting as a heat sink cavity by applying an electric field. The latent heat of solid-liquid phase change can release or absorb a significant amount of energy in a new type of nanofluid called NEPCMs suspension [1]. Several studies have been carried out on natural convection and second law analysis inside various cavities filled with NEPCMs suspension. Ghalambaz et al. [1] investigated the natural convective flow and heat transfer of NEPCMs in a base square cavity. They used the finite element method to discretize and solve the non-dimensional governing equations to understand the critical role of fusion temperature. Aly and Alsedais [2] used incompressible smoothed particle hydrodynamics to simulate double-diffusive convection in a complex-shaped porous cavity suspended by nano-encapsulated phase change materials. They concluded that the Stefan number has a little effect on temperature, concentration, and velocity. The impact of fusion temperature, porous medium, volume concentration of NEPCM, and magnetic field on the heat transfer performance of two complex geometries was explored by Seyyedi et al. [3], [4]. They used CVFEM, a combination of finite element and control volume methods, to solve the governing equations. Mehryan et al. [5] used finite element based CFD software to investigate the mixed convection of NEPCM suspensions in a wavy wall cavity containing a rotating solid cylinder. They concluded that the wall undulation number causes a significant change in the Nusselt number. Shehzad et al. [6] investigated the effect of fin orientation on the natural convection of NEPCM water suspension in a heat exchanger with wing-like fins. The results showed that vertically aligned fins improve thermal performance compared to horizontally aligned fins. Sadeghi et al. [7] studied the natural convection and entropy generation of NEPCMs in an inclined L-shaped cavity. According to the findings, the Stefan number, micro-rotation parameter, and non-dimensional fusion temperature have a negative effect on natural convection heat transfer. Cao et al. [8] used the Finite volume method to investigate the free convection of a mixture of water and NEPCM inside a metal foam porous medium. Adding NEPCM to water increased the average heat flux of the PCM tank. Hussain et al. [9] solved the natural convective flow equations in a nano-encapsulated phase change material suspended in water inside a staggered and grooved porous cavity using FlexPDE software. Almutairi [10] investigated the cooling performance of three integrated circuits in an inclined square cavity filled with NEPCM-water

suspension. Active parameters included Rayleigh number, inclination angle, and NEPCM concentration. Alhashash and Saleh [11] used FlexPDE to investigate the heat transfer in a rotating cavity filled with NEPCM suspension. The results show that at higher rotational speeds, NEPCM experiences less phase change and reduced heat transfer. Fereidooni [12] employed finite element method to numerically analyze natural convection of NEPCM-water suspension in Γ-shaped cavity under the influence of magnetic field. The results showed that the Ha number had a negative effect on the intensity of heat transfer in the NEPCM suspension medium. Using FlexPDE CFD software, Zidan et al. [13] numerically analyzed the natural convection flow and entropy of a NEPCM-water suspension in a reversed T-shaped porous cavity with two hot baffles. They concluded that rising the fusion temperatures cause the expansion and displacement of the melting-freezing zones. In addition to studying the effects of magnetic fields, the researchers also investigated the effects of electric fields on natural convection. Electrodes or surfaces in the cavity were considered by the authors to inject charged particles inside the electric field [14], [15], [16], [17], [18], [19], [20], [21].

Based on the above literature and the stated purpose of this study, we will investigate the natural convection and the second law of thermodynamics in the NEPCM-water suspension enclosure with notched cooling tubes using non-dimensional governing equations in Ansys Fluent with some additional equations for the electric field and electric charge density. Contrary to previous studies that looked at the magnetic field as a moderator of fluid flow and heat transfer, this study looks at the electric field as a possible tool to increase the heat transfer mechanism inside a complex medium. As a result, we show how Rayleigh number, inclination angle, and electric field affect the streamline, isotherm, isoline charge density, and Bejan number in a heat sink cavity filled with NEPCM.

2.Mathematical formulation

2.1 Problem statement

In this paper, we investigate the effect of an electric field on steady laminar natural convection in a NEPCM-water suspension filled heat sink cavity with complex cooling tubes. Each tube has four notches that distort the fluid inside the cavity. Fig. 1 depicts the geometry and mesh of the complex heat sink enclosure with cooling tubes.

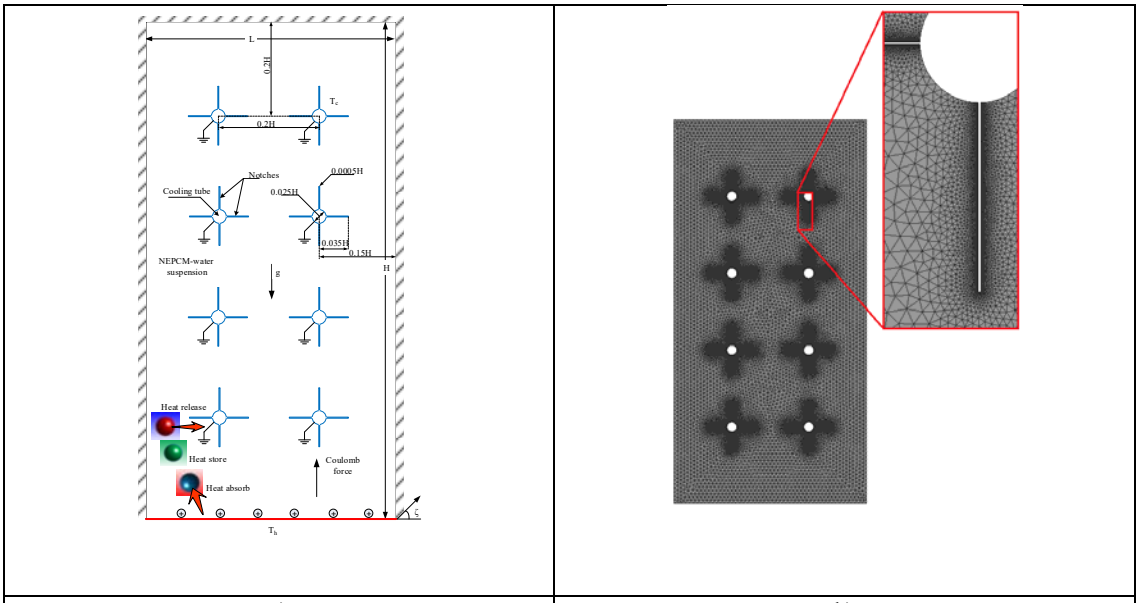

a) b)

Fig. 1. The problem schematic; a) cavity with notched cooling channels, b) Grid view.

In this figure, the characteristic length of the cavity is L, and the cavity height is H, which is twice the length of the cavity. This cavity is chosen because it has a higher heat transfer capability due to its aspect ratio of 2:1 and rectangular shape [22]. Eight complex-shaped cooling tubes inside the cavity remove absorbed heat from the electronic board's bottom wall; all other walls are insulated. The cavity bottom wall and cooling tubes generally remain at fixed temperatures T_0 and T_1 but $T_0 < T_1$. Uniform electric potentials of φ_0 and φ_1 with $\varphi_0 < \varphi_1$ are applied to the collectors (tubes wall) and emitter (bottom wall) electrodes, respectively. In other words, when a voltage φ_1 is applied to the bottom wall electrode, a constant direct current electric field is generated, and the complex shape tube walls act as a grounded electrode, φ_0. As a result, the homogeneous electric charge density, q_1, with charge carrier mobility, K, is injected through the bottom wall into the fluid medium. The magnetic field's effect is ignored due to the electrostatic limit [23].

2.2 Governing equations

Navier-Stokes equations, Maxwell's equations, and Gauss' law are used to derive the equations that govern the flow field. As a result, In the absence of electrical and viscous dissipation, the governing equations are [17], [18]:

$$\nabla.\vec{V} = 0 \tag{1}$$

$$\rho_b(\vec{V}.\nabla)\vec{V} = -\nabla p + \mu_b\nabla^2\vec{V} + (\rho_b - \rho_0)\vec{g} + \vec{F} \tag{2}$$

$$\rho_b c_p(\vec{V}.\nabla)T = k\nabla^2 T + \vec{J}.\vec{E}_0 \tag{3}$$

$$\vec{E}_0 = -\nabla\varphi \tag{4}$$

$$\nabla.(\varepsilon\vec{E}_0) = q \tag{5}$$

$$\nabla.\vec{J} = 0 \tag{6}$$

In Eq. (2), the volumetric electrical body force, $\vec{F}$, is given by (see Ref. [24]):

$$\vec{F}=q\vec{E}_0 - \frac{1}{2}\vec{E}_0^2\,\nabla\varepsilon + \frac{1}{2}\nabla\left(\rho_b\vec{E}_0^2\left(\frac{\partial\varepsilon}{\partial\rho_b}\right)_T\right) \tag{7}$$

The first term on the right-hand side of Eq. (7) is due to the Coulomb force, the second term is due to the inhomogeneity of the permittivity of the dielectric fluid, and the last term is due to the non-uniformity of the electrical permittivity. In general, the second and third terms are the largest contributors to the EHD body force in phase-change processes like boiling, where the EHD body force acts on the liquid-vapor interface [25]. As a result, the last two terms are ignored in the current study. The current density equation is as follows (see Ref. [24]):

$$\vec{J} = \sigma\vec{E}_0 - D\nabla q + q\vec{V} \tag{8}$$

The terms $\sigma\vec{E}_0$, $D\nabla q$, and $q\vec{V}$ in Eq. (8) are the mobility of ion, the diffusion of the charge, and the convection of the charge, respectively. The electric conductivity σ can also be written as $\sigma = Kq$ (see Ref. [26]). Replacing Eqs. (7) - (8) into the main Eqs. (1) - (6), the governing equations are:

$$\frac{\partial u}{\partial x} + \frac{\partial v}{\partial y} = 0 \tag{9}$$

$$u\frac{\partial u}{\partial x} + v\frac{\partial u}{\partial y} = -\frac{1}{\rho_b}\frac{\partial p}{\partial x} + \frac{\mu_b}{\rho_b}\left(\frac{\partial^2 u}{\partial x^2} + \frac{\partial^2 u}{\partial y^2}\right) - g\beta_b(T - T_0)sin\zeta + \frac{1}{\rho_b}qE_{0x} \tag{10}$$

$$u\frac{\partial v}{\partial x} + v\frac{\partial v}{\partial y} = -\frac{1}{\rho_b}\frac{\partial p}{\partial y} + \frac{\mu_b}{\rho_b}\left(\frac{\partial^2 v}{\partial x^2} + \frac{\partial^2 v}{\partial y^2}\right) + g\beta_b(T - T_0)cos\zeta + \frac{1}{\rho_b}qE_{0y} \tag{11}$$

$$u\frac{\partial T}{\partial x} + v\frac{\partial T}{\partial y} = \frac{k_b}{(\rho C_p)_b}\left(\frac{\partial^2 T}{\partial x^2} + \frac{\partial^2 T}{\partial y^2}\right) + \frac{1}{(\rho C_p)_b}\left(Kq\vec{E}_0 - D\nabla q + q\vec{V}\right)\vec{E}_0 \tag{12}$$

$$\vec{E}_0 = -\nabla\varphi \tag{13}$$

$$\nabla.\vec{E}_0 = \frac{q}{\varepsilon} \tag{14}$$

$$\nabla.\left(Kq\vec{E}_0 - D\nabla q + q\vec{V}\right) = 0 \tag{15}$$

The boundary conditions for the above set of equations are as follows.

Hot wall: $u = v = 0, T = T_1, \varphi = \varphi_1, q = q_0$ (16)

Insulated walls: $u = v = 0, \frac{\partial T}{\partial n} = \frac{\partial \varphi}{\partial n} = \frac{\partial q}{\partial n} = 0$

Cooling tube walls: $u = v = 0, T = T_0, \varphi = \varphi_0, \frac{\partial q}{\partial n} = 0$

2.3. characteristics of NEPCM-water suspension

The NEPCM suspension's bulk properties are calculated using [1]:

$$\rho_b = \rho_f(1 - \phi) + \rho_p\phi \tag{17}$$

$$\rho_p = \frac{(1 + \iota)\rho_{co}\rho_{sh}}{\rho_{sh} + \iota\rho_{co}} \tag{18}$$

$$C_{p_b} = \frac{(1-\phi)(\rho C_p)_f + \phi(\rho C_p)_p}{\rho_b} \tag{19}$$

$$\beta_b = \beta_f(1-\phi) + \beta_p\phi \tag{20}$$

$$C_{p_p} = C_{p_{co}} + \left\{\frac{\pi}{2}\left(\frac{h_{sf}}{T_{Mr}} - C_{p_{co}}\right) sin\left(\pi\frac{T-T_0}{T_{Mr}}\right)\right\}\begin{cases} 0 & T < T_{fu} - T_{Mr}/2 \\ 1 & T_{fu} - T_{Mr}/2 < T < T_{fu} + T_{Mr}/2 \\ 0 & T > T_{fu} + T_{Mr}/2 \end{cases} \tag{21}$$

$$\frac{k_b}{k_f} = 1 + N_k\phi \tag{22}$$

$$\frac{\mu_b}{\mu_f} = 1 + N_v\phi \tag{23}$$

2.4 Stream-function-vorticity formulation (Dimensionless forms of the governing equations)

The stream-function-vorticity formulation is utilized to modify a system of non-dimensional equations into a form that can be numerically integrated. The vorticity, stream function, and dimensionless variables are as follows:

$$u = \frac{\partial\psi}{\partial y}, v = -\frac{\partial\psi}{\partial x}, \omega = \frac{\partial v}{\partial x} - \frac{\partial u}{\partial y} \tag{24}$$

$$\mathrm{X} = \frac{x}{H}, \mathrm{Y} = \frac{y}{H}, U = \frac{H}{\alpha_b}u, V = \frac{H}{\alpha_b}v, P = \frac{pH^2}{\rho_b\alpha_b^2}, \Phi = \frac{\varphi-\varphi_0}{\varphi_1-\varphi_0}, Q = \frac{q}{q_0}, \vec{E} = \frac{\vec{E}_0 H}{\varphi_1-\varphi_0}, \tag{25}$$

$$\theta = \frac{T-T_c}{T_h-T_c}, \theta_f = \frac{T_{fu}-T_c}{T_h-T_c}, \Omega = \frac{\omega H^2}{\alpha_b}, \delta = \frac{T_{Mr}}{T_h-T_c}, \Psi = \frac{\psi}{\alpha_b}, \sigma$$

$$= \frac{\left(C_{p_{co}} + \iota C_{p_{sh}}\right)\rho_{co}\rho_{sh}}{(\rho C_p)_f(\rho_{sh} + \iota\rho_{co})}$$

Thus, Eqs. (9)-(15) can be rewritten in non-dimensional forms using Eqs. (24) and (25):

$$\frac{\partial^2\Psi}{\partial \mathrm{X}^2} + \frac{\partial^2\Psi}{\partial \mathrm{Y}^2} = -\Omega \tag{26}$$

$$\left[\frac{\partial\Psi}{\partial \mathrm{Y}}\frac{\partial\Omega}{\partial \mathrm{X}} - \frac{\partial\Psi}{\partial \mathrm{X}}\frac{\partial\Omega}{\partial \mathrm{Y}}\right] \tag{27}$$

$$= \frac{\mu_b/\mu_f}{\rho_b/\rho_f}\mathrm{Pr}_f\left(\frac{\partial^2\Omega}{\partial \mathrm{X}^2} + \frac{\partial^2\Omega}{\partial \mathrm{Y}^2}\right) + \frac{\beta_b}{\beta_f}\mathrm{Ra}_f\mathrm{Pr}_f\left(\frac{\partial\theta}{\partial \mathrm{X}}cos\zeta + \frac{\partial\theta}{\partial \mathrm{Y}}sin\zeta\right)$$

$$+ \frac{\rho_f}{\rho_b}S_E\left[\frac{\partial}{\partial \mathrm{X}}(QE_Y) - \frac{\partial}{\partial \mathrm{Y}}(QE_X)\right]$$

$$\left[\frac{\partial\Psi}{\partial \mathrm{Y}}\frac{\partial\theta}{\partial \mathrm{X}} - \frac{\partial\Psi}{\partial \mathrm{X}}\frac{\partial\theta}{\partial \mathrm{Y}}\right] = \frac{\alpha_b}{\alpha_f}\left(\frac{\partial^2\theta}{\partial \mathrm{X}^2} + \frac{\partial^2\theta}{\partial \mathrm{Y}^2}\right) \tag{28}$$

$$+ S_E E_c\left[\frac{\mathrm{Pr\,Q}}{\mathrm{Pr_E}}(E_X^2 + E_Y^2) - \frac{\frac{D_b}{D_f}}{\frac{(\rho c_p)_b}{(\rho c_p)_f}}\frac{Pr}{D_e}\left(E_X\frac{\partial\mathrm{Q}}{\partial \mathrm{X}} + E_Y\frac{\partial\mathrm{Q}}{\partial \mathrm{Y}}\right) + Q\left(\frac{\partial\Psi}{\partial \mathrm{Y}}E_X - \frac{\partial\Psi}{\partial \mathrm{X}}E_Y\right)\right]$$

$$\frac{\partial^2\Phi}{\partial \mathrm{X}^2} + \frac{\partial^2\Phi}{\partial \mathrm{Y}^2} = -N_E Q \tag{29}$$

$$\left[\frac{\partial \Psi}{\partial Y}\frac{\partial Q}{\partial X}-\frac{\partial \Psi}{\partial X}\frac{\partial Q}{\partial Y}\right]+\frac{\mathrm{Pr}}{\mathrm{Pr_E}}\left[Q\left(\frac{\partial E_X}{\partial X}+\frac{\partial E_Y}{\partial Y}\right)+E_X\frac{\partial Q}{\partial X}+E_Y\frac{\partial Q}{\partial Y}\right]=\frac{Pr}{D_e}\left(\frac{\partial^2 Q}{\partial X^2}+\frac{\partial^2 Q}{\partial Y^2}\right) \quad (30)$$

Where Ra_f, Pr_f, S_E, E_c, Pr_E, N_E and D_e are defined as follows:

$$\mathrm{Ra}_f=\frac{g\beta_f H^3(T_h-T_c)}{\nu_f\alpha_f},\mathrm{Pr}_f=\frac{\nu_f}{\alpha_f},E_c=\frac{\alpha_f^2}{c_p H^2(T_h-T_c)},\ \mathrm{Pr}_E=\frac{\nu_f}{K(\varphi_1-\varphi_0)}\ , \quad (31)$$

$$N_E=\frac{q_0 H^2}{\varepsilon(\varphi_1-\varphi_0)},D_e=\frac{\nu_f}{D}$$

The heat capacity ratio is defined as:

$$C_r=\frac{C_{p_b}\rho_b}{C_{p_f}\rho_f}=(1-\phi)+\phi\sigma+\frac{\phi}{\delta Ste}\left\{\frac{\pi}{2}sin\left(\frac{\pi}{\delta}\left(\theta-\theta_{fu}+\frac{\delta}{2}\right)\right)\right\}\begin{cases}0 & \theta<\theta_{fu}-\delta/2\\ 1 & \theta_{fu}-\delta/2<\theta<\theta_{fu}+\delta/2\\ 0 & \theta>\theta_{fu}+\delta/2\end{cases} \quad (32)$$

The boundary conditions by considering stream-vorticity in non-dimensional formulation take the form:

$$\text{Hot wall: } \Psi=\frac{\partial \Psi}{\partial Y}=0,\theta=1,\Phi=1,Q=1 \quad (33)$$

$$\text{Insulated walls: } \Psi=\frac{\partial \Psi}{\partial Y}=0,\frac{\partial \theta}{\partial n}=\frac{\partial \Phi}{\partial n}=\frac{\partial Q}{\partial n}=0$$

$$\text{Cooling tube walls: } \Psi=\frac{\partial \Psi}{\partial Y}=0,\theta=0,\varphi=0,\frac{\partial Q}{\partial n}=0$$

2.5 Nusselt number

The indicators of heat transfer rate in the cavity are calculated by $\mathrm{Nu_{ave}}$ in the cavity and Nu_{local} (local Nusselt number) on the hot bottom wall:

$$\mathrm{Nu}_{local,x}=-\left(\frac{k_\gamma}{k_f}\right)\frac{\partial \theta}{\partial Y}\,|_{Y=0} \quad (34)$$

$$\mathrm{Nu_{ave}}=\frac{1}{S}\int_0^S \mathrm{Nu}_{local}\,dS=-2\int_0^{0.5}\mathrm{Nu}_{local}\,|_{Y=0}dX \quad (35)$$

2.6 Second law of thermodynamics analysis

The rate of entropy generation can be calculated as follows:

$$\dot{S}_{\mathrm{gen}}=\frac{k_\gamma}{T_0^2}\left[\left(\frac{\partial T}{\partial x}\right)^2+\left(\frac{\partial T}{\partial y}\right)^2\right]+\frac{\mu_\gamma}{T_0}\left[2\left(\frac{\partial u}{\partial x}\right)^2+2\left(\frac{\partial v}{\partial y}\right)^2+\left(\frac{\partial u}{\partial y}+\frac{\partial v}{\partial x}\right)^2\right]+\frac{Kq(E_{0X}^2+E_{0Y}^2)}{T_0} \quad (36)$$

The heat transfer, viscous dissipation, and electric field all contribute to the generation of local entropy in Eq. (36). In non-dimensional form, the local entropy generation is as follows:

$$N_{L,gen} = \frac{\dot{S}_{gen}}{\left[\left(\frac{k_f}{T_0^2}\right)\left(\frac{T_h - T_c}{L}\right)^2\right]} = \frac{k_\gamma}{k_f}\left[\left(\frac{\partial\theta}{\partial X}\right)^2 + \left(\frac{\partial\theta}{\partial Y}\right)^2\right] + \frac{\mu_\gamma}{\mu_f}\Phi_f\left[4\left(\frac{\partial^2\Psi}{\partial X\,\partial Y}\right)^2 + \left(\frac{\partial^2\Psi}{\partial Y^2} - \frac{\partial^2\Psi}{\partial X^2}\right)^2\right] + \frac{S_E}{Pr_E}\Phi_f Q\left[\left(\frac{\partial\Phi}{\partial X}\right)^2 + \left(\frac{\partial\Phi}{\partial Y}\right)^2\right] \quad (37)$$

$$\Phi_f = \frac{\mu_f T_0}{k_f}\left(\frac{\alpha_f}{L\Delta T}\right)^2 \quad (38)$$

The Eq. (37) can be generalized as:

$$N_{L,gen} = N_{L,HT} + N_{L,FF} + N_{L,EF} \quad (39)$$

The first term is the entropy generation due to heat transfer, the second term is for fluid friction and the last term is the influence of the electric field. In this study, the second law of thermodynamics is evaluated by calculating the local Bejan number which represents the strength of the entropy generation due to heat transfer irreversibility to the overall entropy generation [27], [28]:

$$Be_L = N_{L,HT}/N_{L,gen} \quad (40)$$

The average Bejan number is:

$$Be_{ave} = \frac{\int_A Be_L(X,Y)dA}{\int_A dA} \quad (41)$$

3. Numerical details

3.1 Numerical method

Natural convection and entropy generation are simulated by ANSYS Fluent academic version CFD code with an integrated non-dimensionalization scheme. The governing equations are discretized using a pressure-based finite volume method. Since the buoyancy term is treated by the Boussinesq approximation [29], the temperature variations of fluid properties are neglected. Wall boundaries are assumed to be smooth and without roughness. The COUPLED algorithm is used to couple the pressure and velocity fields. The PRESTO scheme is employed for spatial pressure discretization [30] and second-order upwind applied to the formulation of the convection contribution to the coefficients in the finite-volume equations The convergence criterion for conservation equations is 10^{-6}. The electric effect is introduced by the potential equation and the charge density equation as two user-defined scalars (UDS) with exclusive user-defined functions to cover the source terms of the equations. The boundary conditions also considered the effects of electric potential and charge density through UDS values in the walls. Two user-defined functions are used to couple the electric field as source terms for momentum equations. Custom functions are used to compute entropy generation and

the Bejan number. The pressure-based finite volume approach is utilized to discretize the governing equations. Except for the Boussinesq approximation's buoyancy factor.

3.2 Grid check

The mesh sensitivity study for NEPCM-water suspension without electric field at Ra=10^4 and ζ =90° was performed to determine the proper cavity mesh. As shown in Fig. 2, a mesh of 265894 or finer is suitable for the grid-independent solution and diminishing discretization errors in numerical simulation.

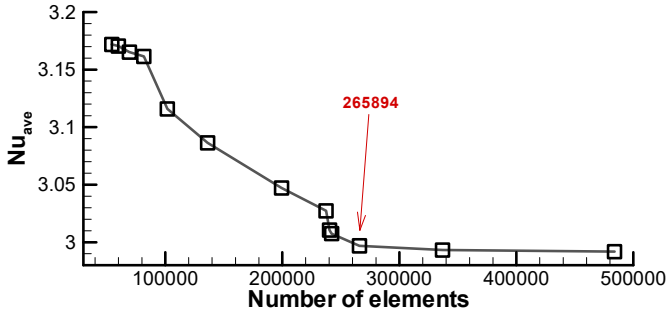

Fig. 2. Convergence of the Nu_{ave} at the bottom hot wall with successive mesh refinement.

3.3 Validation of the numerical approach

The numerical method has been validated utilizing using the numerical data of Yang and Ordonez's [31]. However, when the modified Ra is considered, there is no exact test case that is similar to problem cooling tubes. Warrington and Powe [32] presented experimental results for air free convection between a hot cylindrical body with radius R and its cold square enclosure with length L. They calculated Ra and Nu using a hypothetical gap width L defined as the distance between an imaginary outer sphere with the volume of a cube and an imaginary inner sphere with the volume of a cylinder. The average Nusselt number recomputed with modified Rayleigh number, Ra_L, for an aspect ratio of 0.2 as shown in Table 1. Our findings are consistent with those of Yang and Ordonez [31]. In addition to checking the validity of the model, the contours of the isotherms and streamlines were compared to those contours that presented in references [31], [32] (Fig. 3).

Table 1. Validation the numerical method

Ra	Ra_L	present study	Warrington and Powe [32]	Yang and Ordonez [31]	percent error related to Ref. [31]
10^4	1.114×10^4	5.156	5.286	5.156	0%
10^5	1.114×10^5	8.07	8.67	8.06	-0.12%
10^6	1.114×10^6	14.56	14.229	14.49	-0.48%

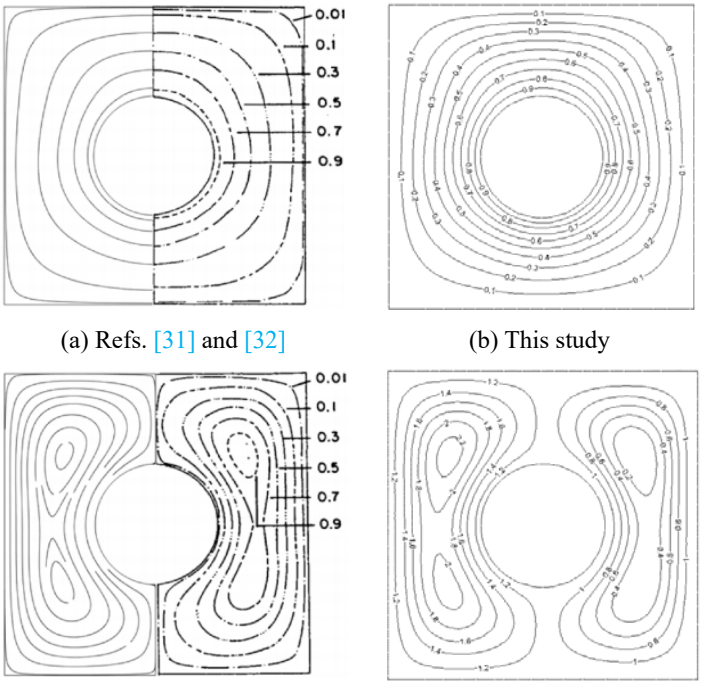

(a) Refs. [31] and [32] (b) This study

(c) Refs. [31] and [32] **(d) This study**

Fig. 3. Comparison of isotherms (a, b) and streamlines (c, d) obtained with this study and from references (Ref. [31] (solid lines) and Ref. [32] (dashed lines)) at Ra=10^4

4. Results and discussion

This study investigates natural convection heat transfer and entropy generation in a complex cavity filled with NEPCM-water suspension with notched cooling tubes subjected to an external electric field. The suspension of the base fluid and NEPCM is considered as a diluted suspension. NEPCM particles have a shell of polymethyl methacrylate (PMMA) and a core of n-octadecane [33]. For simplicity, dielectric permittivity and ionic mobility are assumed to be constant. The main forces that govern the fluid flow are the Coulomb force and the buoyancy force. The buoyancy force is changed due to inclination of the cavity ($\zeta = 45°$ and $90°$), but the Coulomb force is fixed between bottom wall and the tubes for Rayleigh number 10^3-10^5. The results are presented in the form of isotherms, streamlines, isolines of electric charge density, Bejan number, heat capacity ratio, and Nusselt number. Table 2 lists the non-dimensional parameters used.

Table 2: The default values of the dimensionless parameters

Pr_f	θ_{fu}	Pr_E	ϕ	σ	Φ	N_E	Ste	N_k	N_v	ρ_p/ρ_f	D_e	δ	E_C	$\phi \times \beta_p/\beta_f$
6.2	0.5	1	0.02	0.4	10^{-4}	1	0.2	3	6	0.9	1	0.05	1	0

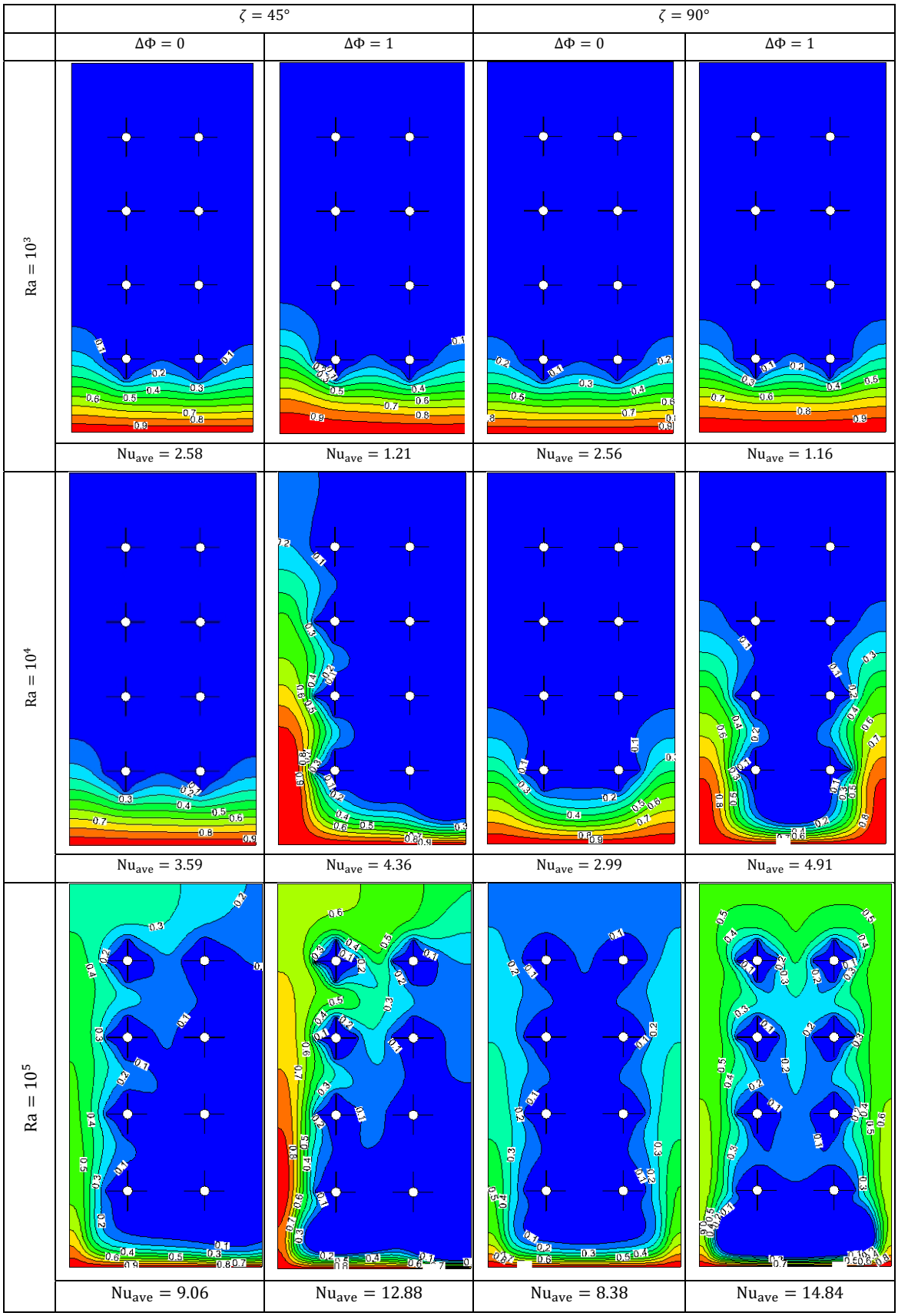

Fig. 4. The contours of isotherms for NEPCM-filled cavity with and without electric field

The results of isotherms contours, local and average Nusselt number, stream function, the Bejan number, isoline of electric charge, and heat capacity ratio for NEPCM-water suspension in complex heat sink cavity under normal condition and electric field conditions are shown in Figs. 4-9. Fig. 4 illustrates the isotherm contours for a range of laminar Rayleigh numbers, inclined cavity ($\zeta = 45°$), and straight cavity ($\zeta = 90°$) with ($\Delta\Phi = 1$) and without electric field ($\Delta\Phi = 0$). The fluid flow inside the notch as shown in Fig. 1 are no longer clear due to the smaller size of the figure. But the effect of the notches is significant.

According to Fig. 4 and Fig. 5, the Nu_{ave} and Ψ_{max} increase with Ra and electric field. However, by applying an electric field to the fluid of the cavity at $Ra=10^3$ the heat transfer decreased due to the saturation charge effect of electric charges which strongly injected from the hot wall (bottom wall). In other words, we need a threshold of Rayleigh number to apply an effective electric field. In Fig. 8 this negative effect is apparent for $Ra=10^3$ where the electric charge bands are wider than in the other cases with higher Rayleigh number. The values of Nu_{ave} increase in the presence of electrical field for $Ra=10^4$ and $Ra=10^5$ because the coulomb force and the bouncy force are in the same direction. In fact, the electric field strengthens the convection flow. But at $Ra=10^3$, convection flow is weak, so the Coulomb force cannot contribute significantly to the heat transfer enhancement. The effect of inclination angle is different. Under normal condition, the Nu decreases with the increase of the inclination angle from 45º to 90º, but in the presence of an electric field, Nu increases. For example, in $Ra=10^4$ the Nusselt number increases by 21.41% for $\zeta = 45°$, and 64.21% for $\zeta = 90°$ and for $Ra=10^5$ these values increase by 42.16% and 77.08%, respectively. It is interesting that in the presence of an electric field, the Nusselt number increases by 202.25% at $\zeta = 90°$ when the Rayleigh number rises from $Ra=10^4$ to $Ra=10^5$. In fact, the thickness of thermal boundary-layer decreases with increase of the Rayleigh number and therefore, the heat transfer coefficient and Nusselt number increase.

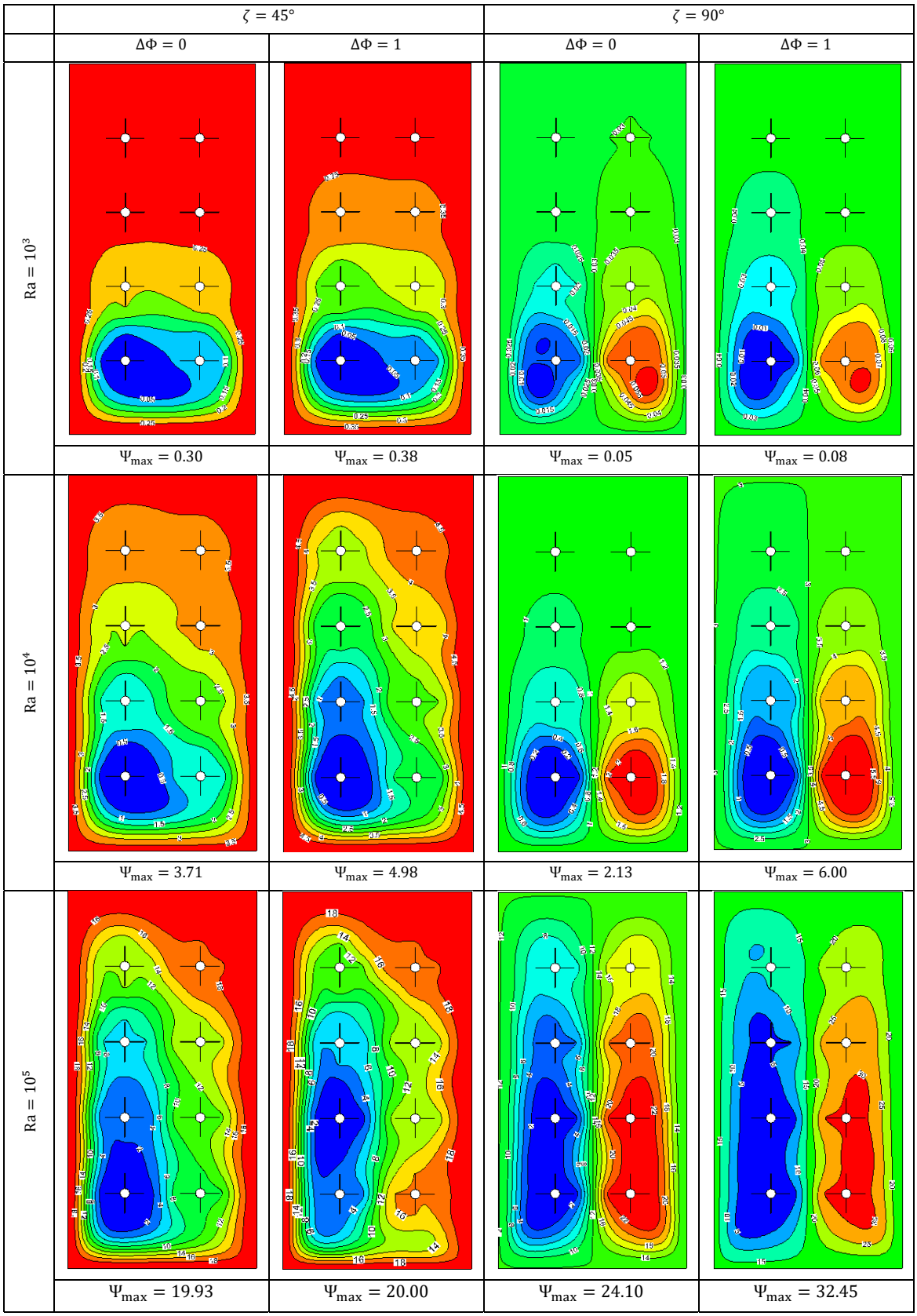

Fig. 5. The contours of streamlines for NEPCM-filled cavity with and without electric field

From Fig. 5, it is clear that with the increase of Ra and the application of the electric field, the maximum stream function increases. This means that the fluid flows at a higher velocity to transfer the applied heat from the electronic devices to the cooling tubes. However, at Ra=10^3 for this complex cavity, it seems that the density of electric charge injection is not enough to provide the required Coulomb force to increase heat transfer from the bottom wall to the top wall of the cavity and the upper cooling tubes. According to the last term in momentum equation (Eq. (27)), this term has a positive value that can help to increase the fluid velocity and therefore the values of Ψ_{max} increase. For $\zeta = 45°$ there is only one center of vortices which is formed around the first cooling tube according to slope direction. For $\zeta = 90°$, there are two vortex centers due to the same fluid passing between the cooling tubes up and down. Moreover, by applying the electric field, the center of vortices was strengthened and moved upwards. It is clear from the figure that for $\zeta = 45°$, the center of vortices shifted up (around the second raw of the cooling tubes) and for $\zeta = 90°$, the maximum stream function has increased by about 34.6%. Fig. 6 shows the local and the average Bejan numbers inside the cavity with and without the influence of the electric field. Due to the irreversibility of fluid friction and heat transfer the Bejan number has an inverse relationship with the Rayleigh number. Contrary to previous studies about magnetic field [27], [28], with the application of electric field, the Bejan number increases due to irreversibility of the heat transfer. Indeed, in the presence of an electric field, both the first and third terms in the RHS of Eq. (37) increase, but the increasing in the first term (due to the irreversibility of heat transfer) is more than that of last term (due to the irreversibility of electric field). At low Ra, specifically Ra=10^3 and $\zeta = 90°$, the local Bejan number is close to one due to the dominant conduction heat transfer mechanism in most regions. At Ra=10^5, part of the irreversibility of heat transfer is reduced due to minimizing the heat transfer irreversibility. The electric field has no significant effect on the Bejan number at this Ra. For example, in Ra=10^5 and $\zeta = 90°$ the average Bejan number has increased by 16.66%.

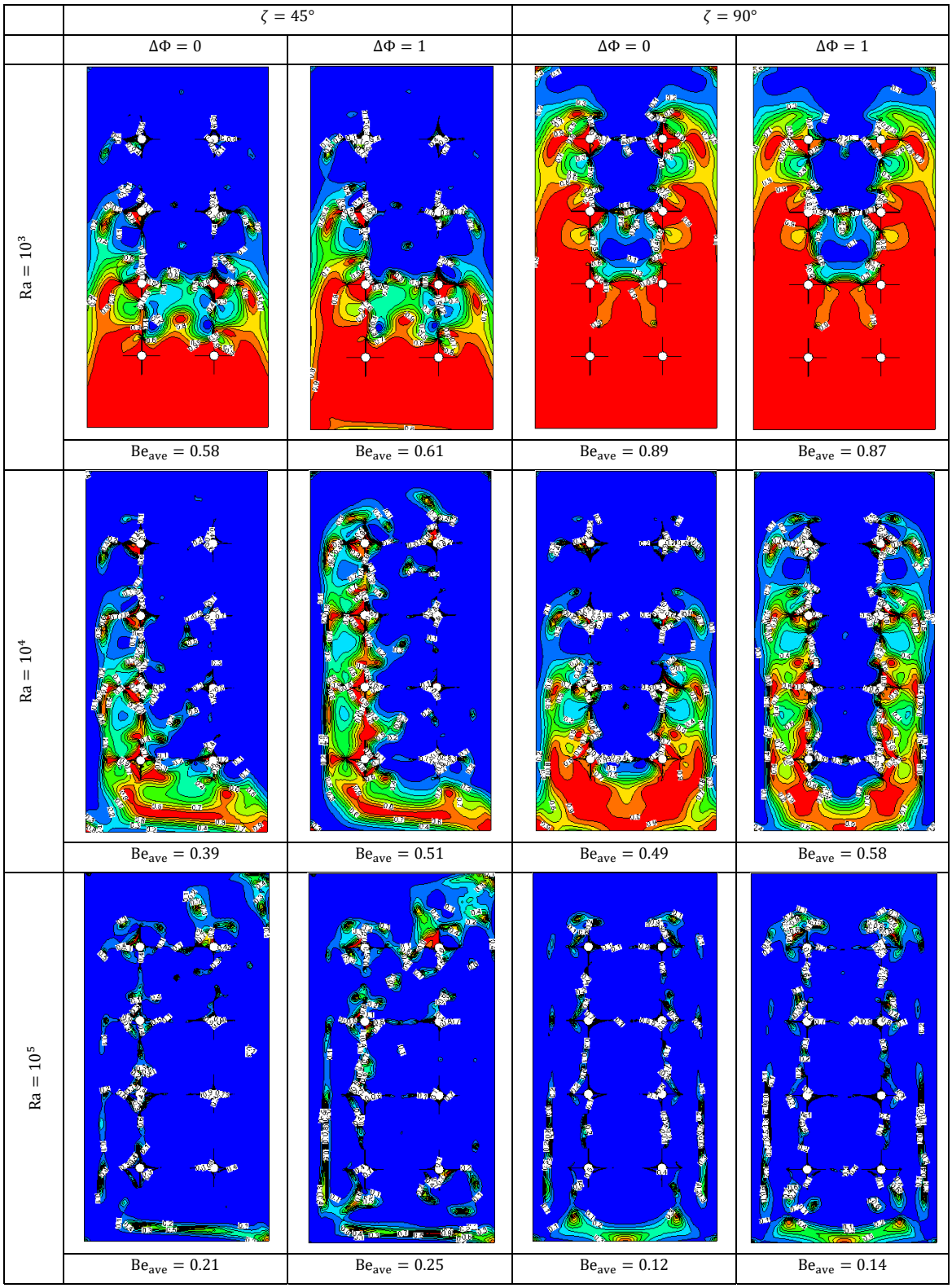

Fig. 6 The contours of local Bejan number for NEPCM-filled cavity with and without electric field

Fig. 7 shows the effects of Rayleigh number, inclination angle and electric field on the heat capacity ratio (Cr). In the red region, the nano-encapsulated phase change particles undergo phase change

within their capsules where the phase change move toward the cooling walls. It is obvious that the phase change occurred in a wider region at Ra=10^5 for $\zeta = 45°$and $\zeta = 90°$. As it is known, the values of Ψ_{max} and Nu_{ave} increase with the increase of the Rayleigh number, and as a result, the heat transfer rate and the fluid flow rate increase, which leads to an increase in the phase change rate.

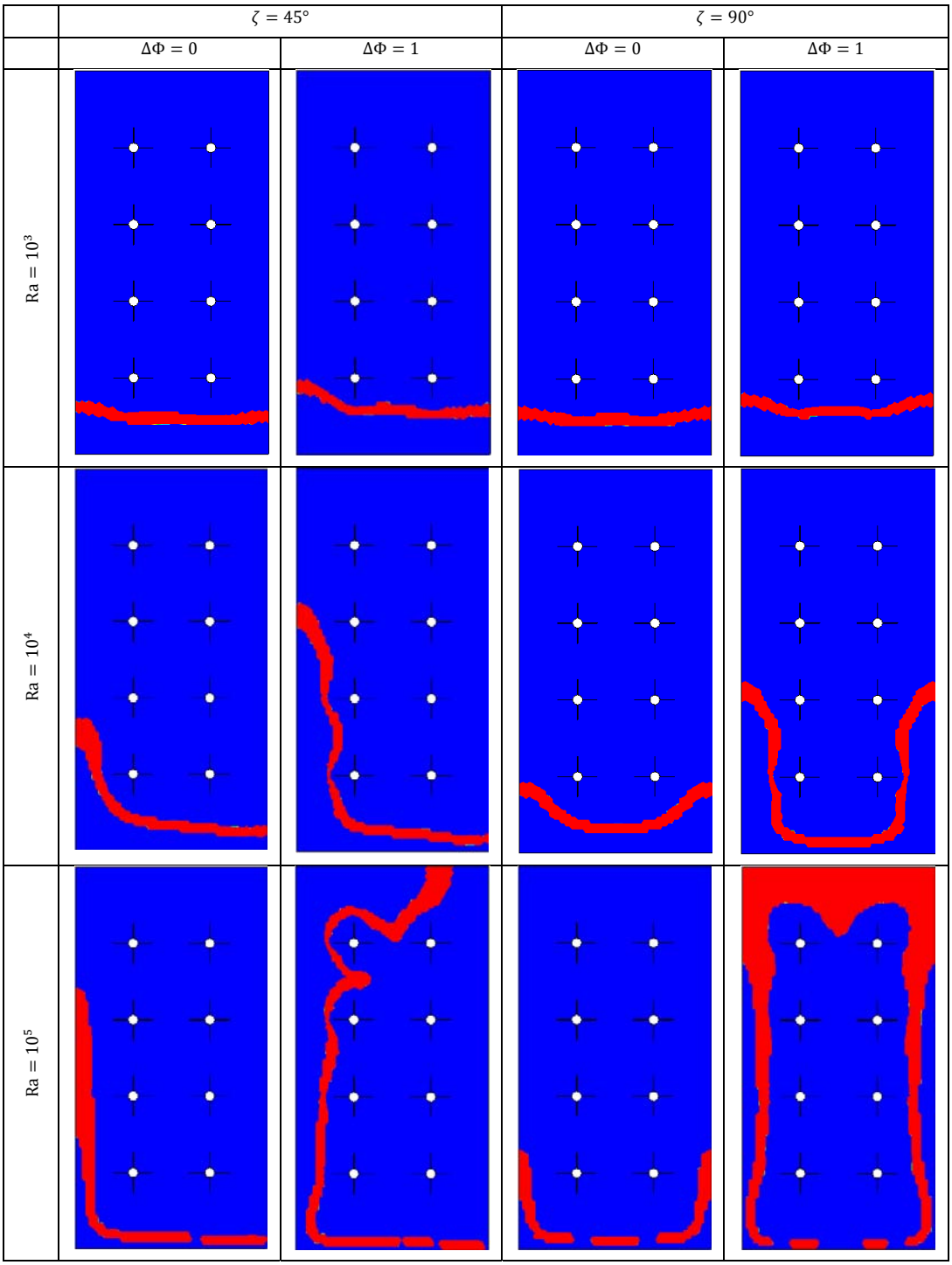

Fig. 7. The effects of Rayleigh number, inclination angle, and electric field on the heat capacity ratio.

Isolines of electrical density are presented in Fig. 8. It is clear that the Ra augments the distortion of isoelectric density Nevertheless, in the case of low Ra, the Lorentz force is insufficient to influence the fluid flow; in contrast, with high Ra, the fluid flow is enhanced due to the greater influence of the electric field. At $\zeta = 90°$, the isoline of electrical density affect the fluid flow symmetrically, so almost the entire cavity is affected by the electric field.

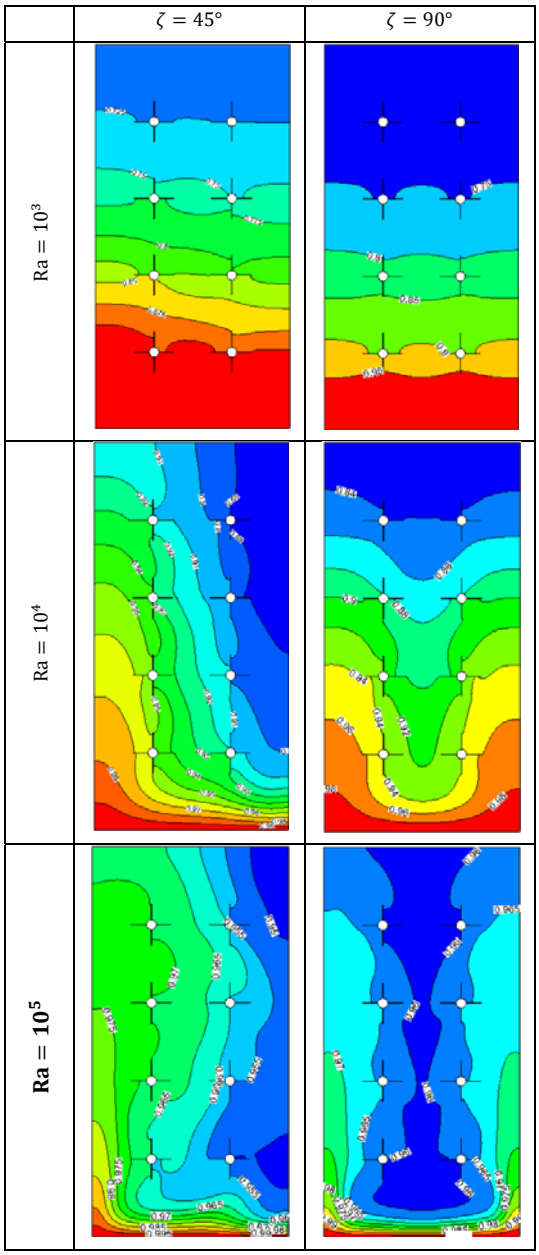

Fig. 8 The contours of electric density distribution that injected by the bottom electrode

Fig. 9 shows the Nu_{local} variations alongside the bottom hot wall of the enclosure for two inclination angles of the cavity. The increase of the Nusselt number means that the temperature gradient has increased. Therefore, the heat transfer between the heated wall and fluid is enhanced.

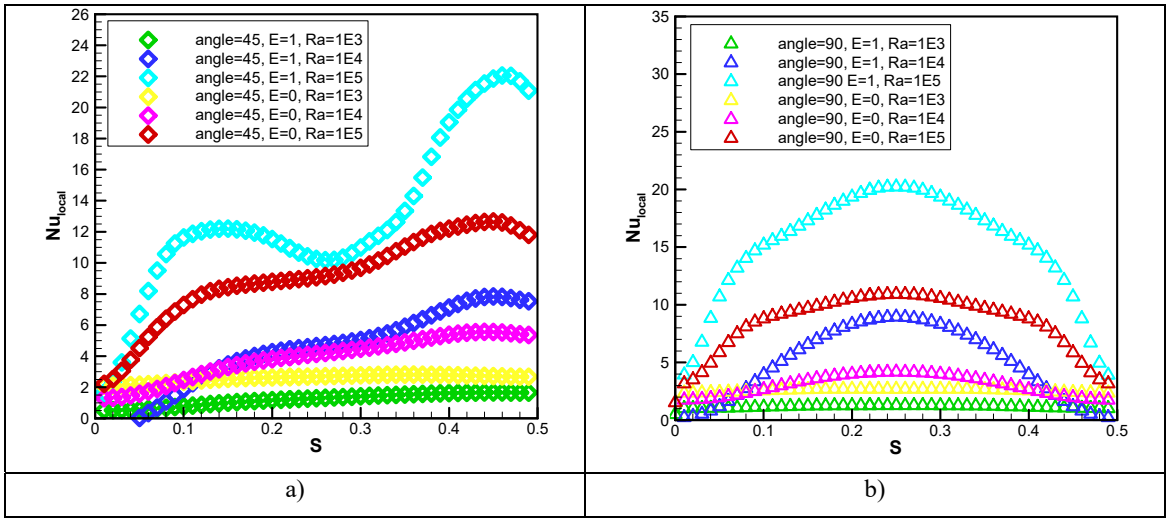

a) b)

Fig. 9 Influences of Ra, and electric field on Nu_{local} with; a) $\zeta = 45°$, $\zeta = 90°$

It is clear that Nu_{local} boosts as Ra and electric field. In general, the highest heat transfer is near the cooling boundaries, so for $\zeta = 45°$, Nu_{local} has high peak due to inclination (Fig. 9a), and at $\zeta = 90°$ there is a maximum Nusselt number (Fig. 9b) which is located between two cooling tubes. Among the cases, the effect of the electric field at $Ra=10^5$ is so high that the fluid defect is significant.

5. Conclusion

Simulation by ANSYS Fluent was addressed in this study to explain the characteristics of heat transfer, free convection, and entropy generation. In addition to the mass, momentum, and energy equations, two additional equations with associated boundary conditions are programmed to fully account for the effect of the electric field. A parametric study was performed for various parameters, e.g., Rayleigh number, inclination angle, and electric field. The enclosure is cooled by eight cooling channels. The cavity is filled with NEPCM-water suspension. The contribution of the latent heat energy absorption and release of NEPCM nanoparticles owing to phase change is considered. The results for vorticity, isotherms, local and average Nusselt number, and Bejan number were expressed and discussed. The main conclusions can be summarized as follows:

- The ability of the finite volume method integrated into ANSYS Fluent to investigate a complex problem can be proven due to an excellent agreement in the validation process.
- The results show that Nu_{ave} boosts with increasing Rayleigh number (Fig. 4). The conclusions also state that in complex geometries, higher Ra facilitates heat transfer in all regions.
- It is proposed to use the electric field as a heat transfer tool since convective heat transfer is enhanced with the electric field.
- Be_{ave} increases with electric field and diminishes with Ra. The Be_{ave} at low Rayleigh number indicates that conductive heat transfer mechanism is the dominant mode of heat transfer.
- The fluid flow and heat transfer at $Ra=10^5$ and inclination angle 90º is the best (Fig. 4-9).

References:

[1] M. Ghalambaz, A. J. Chamkha, and D. Wen, "Natural convective flow and heat transfer of Nano-Encapsulated Phase Change Materials (NEPCMs) in a cavity," *Int. J. Heat Mass Transf.*, vol. 138, pp. 738–749, 2019, doi: 10.1016/j.ijheatmasstransfer.2019.04.037.

[2] A. M. Aly and N. Alsedais, "Double-diffusive convection in a porous complex-shaped cavity suspended by nano-encapsulated phase change materials," *ZAMM Zeitschrift fur Angew. Math. und Mech.*, vol. 101, no. 11, 2021, doi: 10.1002/zamm.202000376.

[3] S. M. Seyyedi, M. Hashemi-Tilehnoee, and M. Sharifpur, "Effect of inclined magnetic field on the entropy generation in an annulus filled with NEPCM suspension," *Math. Probl. Eng.*, vol. 2021, 2021, doi: 10.1155/2021/8103300.

[4] S. M. Seyyedi, M. Hashemi-Tilehnoee, and M. Sharifpur, "Impact of Fusion Temperature on Hydrothermal Features of Flow within an Annulus Loaded with Nanoencapsulated Phase Change Materials (NEPCMs) during Natural Convection Process," *Math. Probl. Eng.*, vol. 2021, 2021, doi: 10.1155/2021/4276894.

[5] S. A. M. Mehryan *et al.*, "Latent heat phase change heat transfer of a nanoliquid with nano–encapsulated phase change materials in a wavy-wall enclosure with an active rotating cylinder," *Sustain.*, vol. 13, no. 5, pp. 1–20, 2021, doi: 10.3390/su13052590.

[6] S. A. Shehzad, B. Alshuraiaan, M. S. Kamel, M. Izadi, and T. Ambreen, "Influence of fin orientation on the natural convection of aqueous-based nano-encapsulated PCMs in a heat exchanger equipped with wing-like fins," *Chem. Eng. Process. - Process Intensif.*, vol. 160, 2021, doi: 10.1016/j.cep.2020.108287.

[7] M. S. Sadeghi, A. J. Chamkha, R. Ali, M. B. Ben Hamida, M. Ghodrat, and A. M. Galal, "Hydrothermal behavior of micro-polar Nano-Encapsulated phase change materials (NEPCMs) in an inclined L-shaped cavity," *Case Stud. Therm. Eng.*, vol. 35, p. 102039, 2022, doi: 10.1016/j.csite.2022.102039.

[8] Y. Cao *et al.*, "Receiving heat from a PCM tank by using natural convection of water and NEPCM: A simulation for LHTES application," *Case Stud. Therm. Eng.*, vol. 35, p. 102123, 2022, doi: 10.1016/j.csite.2022.102123.

[9] S. Hussain, M. Molana, T. Armaghani, A. M. Rashad, and H. A. Nabwey, "Energy storage performance and irreversibility analysis of a water-based suspension containing nano-encapsulated phase change materials in a porous staggered cavity," *J. Energy Storage*, vol. 53, p. 104975, 2022, doi: 10.1016/j.est.2022.104975.

[10] K. Almutairi, “Cooling three integrated circuits by embedding them inside an inclined cavity using nano-encapsulated phase change material,” *J. Energy Storage*, vol. 52, p. 104837, 2022, doi: 10.1016/j.est.2022.104837.

[11] A. Alhashash and H. Saleh, “Free convection flow of a heterogeneous mixture of water and nano-encapsulated phase change particle (NEPCP) in enclosure subject to rotation,” *J. Energy Storage*, vol. 51, p. 104168, 2022, doi: https://doi.org/10.1016/j.est.2022.104168.

[12] J. Fereidooni, “Heat transfer inspection of nano-encapsulated phase change materials inside a Γ-shaped enclosure influenced by magnetic field,” *J. Magn. Magn. Mater.*, vol. 561, p. 169682, 2022, doi: 10.1016/j.jmmm.2022.169682.

[13] A. M. Zidan *et al.*, “Thermal management and natural convection flow of nano encapsulated phase change material (NEPCM)-water suspension in a reverse T-shaped porous cavity enshrining two hot corrugated baffles: A boost to renewable energy storage,” *J. Build. Eng.*, vol. 53, p. 104550, 2022, doi: 10.1016/j.jobe.2022.104550.

[14] M. Sheikholeslami, S. A. Shehzad, and R. Kumar, “Natural Convection of Fe3O4-Ethylene Glycol Nanouid under the Impact of Electric Field in a Porous Enclosure,” *Commun. Theor. Phys.*, vol. 69, no. 6, pp. 667–675, 2018, doi: 10.1088/0253-6102/69/6/667.

[15] M. Sheikholeslami and M. Seyednezhad, “Simulation of nanofluid flow and natural convection in a porous media under the influence of electric field using CVFEM,” *Int. J. Heat Mass Transf.*, vol. 120, 2018, doi: 10.1016/j.ijheatmasstransfer.2017.12.087.

[16] T. F. Li, J. Wu, K. Luo, and H. L. Yi, “Lattice Boltzmann simulation of electro-hydro-dynamic (EHD) natural convection heat transfer in horizontal cylindrical annuli,” *Int. Commun. Heat Mass Transf.*, vol. 98, pp. 106–115, 2018, doi: 10.1016/j.icheatmasstransfer.2018.08.014.

[17] N. C. Roy, L. K. Saha, and S. Siddiqa, “Electrohydrodynamics and thermal radiation effects on natural convection flow in an enclosed domain,” *Int. Commun. Heat Mass Transf.*, vol. 126, 2021, doi: 10.1016/j.icheatmasstransfer.2021.105437.

[18] N. C. Roy, F. Yesmin, L. K. Saha, and S. Siddiqa, “Electrohydrodynamics natural convection flow of nanofluids in a rectangular cavity enclosed by a corrugated bottom surface,” *Fluid Dyn. Res.*, vol. 53, no. 1, 2021, doi: 10.1088/1873-7005/abe216.

[19] S. S. M. Golsefid, N. Amanifard, H. M. Deylami, and F. Dolati, “Numerical and experimental study on EHD heat transfer enhancement with Joule heating effect through a rectangular enclosure,” *Appl. Therm. Eng.*, vol. 123, pp. 689–698, 2017, doi: 10.1016/j.applthermaleng.2017.05.129.

[20] Y. S. Daniel, Z. A. Aziz, Z. Ismail, and F. Salah, "Numerical study of entropy analysis for electrical unsteady natural magnetohydrodynamic flow of nanofluid and heat transfer," *Chinese J. Phys.*, vol. 55, no. 5, pp. 1821–1848, 2017, doi: 10.1016/j.cjph.2017.08.009.

[21] W. Hassen, H. F. Oztop, L. Kolsi, M. N. Borjini, and N. Abu-Hamdeh, "Analysis of the electro-thermo-convection induced by a strong unipolar injection between two concentric or eccentric cylinders," *Numer. Heat Transf. Part A Appl.*, vol. 71, no. 7, pp. 789–804, 2017, doi: 10.1080/10407782.2017.1308725.

[22] C. Qi, C. Li, K. Li, and D. Han, "Natural convection of nanofluids in solar energy collectors based on a two-phase lattice Boltzmann model," *J. Therm. Anal. Calorim.*, vol. 147, no. 3, pp. 2417–2438, 2022, doi: 10.1007/s10973-021-10668-8.

[23] P. J. Martin and A. T. Richardson, "Conductivity models of electrothermal convection in a plane layer of dielectric liquid," *J. Heat Transfer*, vol. 106, no. 1, pp. 131–136, 1984, doi: 10.1115/1.3246625.

[24] T. Fujino, Y. Yokoyama, and Y. H. Mori, "Augmentation of laminar forced- convective heat transfer by the application of a transverse electric field," *J. Heat Transfer*, vol. 111, no. 2, pp. 345–351, 1989, doi: 10.1115/1.3250683.

[25] E. Monajjemi Rarani, N. Etesami, and M. Nasr Esfahany, "Influence of the uniform electric field on viscosity of magnetic nanofluid (Fe3O4-EG)," *J. Appl. Phys.*, vol. 112, no. 9, 2012, doi: 10.1063/1.4763469.

[26] V. G. Babskii, M. Y. Zhukov, and V. I. Yudovich, *Mathematical Theory of Electrophoresis*. Springer Science & Business Media, 1988. doi: 10.1007/978-1-4613-0879-9.

[27] M. Hashemi-Tilehnoee, E. P. del Barrio, and S. M. Seyyedi, "Magneto-turbulent natural convection and entropy generation analyses in liquid sodium-filled cavity partially heated and cooled from sidewalls with circular blocks," *Int. Commun. Heat Mass Transf.*, vol. 134, p. 106053, 2022, doi: 10.1016/j.icheatmasstransfer.2022.106053.

[28] M. Hashemi-Tilehnoee, A. S. Dogonchi, S. M. Seyyedi, and M. Sharifpur, "Magneto-fluid dynamic and second law analysis in a hot porous cavity filled by nanofluid and nano-encapsulated phase change material suspension with different layout of cooling channels," *J. Energy Storage*, vol. 31, 2020, doi: 10.1016/j.est.2020.101720.

[29] M. Hashemi-Tilehnoee, S. Tashakor, A. S. Dogonchi, S. M. Seyyedi, and M. Khaleghi, "Entropy generation in concentric annuli of 400 kV gas-insulated transmission line," *Therm. Sci. Eng. Prog.*, vol. 19, 2020, doi: 10.1016/j.tsep.2020.100614.

[30] Hashemi-Tilehnoee, M. and del Barrio, E.P., 2022. Magneto laminar mixed convection and entropy generation analyses of an impinging slot jet of Al2O3-water and Novec-649. Thermal Science and Engineering Progress, p.101524.

[31] S. Yang and J. C. Ordonez, "Optimal cooling channel layout in a hot enclosure subject to natural convection," *J. Heat Transfer*, vol. 141, no. 11, 2019, doi: 10.1115/1.4044510.

[32] R. O. Warrington and R. E. Powe, "The transfer of heat by natural convection between bodies and their enclosures," *Int. J. Heat Mass Transf.*, vol. 28, no. 2, pp. 319–330, 1985, doi: 10.1016/0017-9310(85)90065-1.

[33] Y. Rao, F. Dammel, P. Stephan, and G. Lin, "Convective heat transfer characteristics of microencapsulated phase change material suspensions in minichannels," *Heat Mass Transf. und Stoffuebertragung*, vol. 44, no. 2, pp. 175–186, 2007, doi: 10.1007/s00231-007-0232-0.